



## Supplementary Materials

**Table S1.** Physical properties of LaFeO<sub>3</sub> and LaMnO<sub>3</sub>.

Sample	BET surface area (m <sup>2</sup> ·g <sup>-1</sup> )	Average pore volume (cm <sup>3</sup> ·g <sup>-1</sup> )	Average pore diameter (nm)
LaFeO <sub>3</sub>	3.35	0.039	36.22
LaMnO <sub>3</sub>	12.67	0.042	14.84

**Table S2.** Adsorption isotherm constants of LaMnO<sub>3</sub>.

Initial concentration (mg/L)	Dosage (g)	Equilibrium concentration C <sub>e</sub> (mg/L)	Adsorption capacity q <sub>e</sub> (mg/g)	C <sub>e</sub> /q <sub>e</sub> (g/L)	lgC <sub>e</sub>	lgq <sub>e</sub>
5	0.1	0.34	23.28	0.01	-0.47	1.37
7.5	0.1.	1.16	31.70	0.04	0.06	1.50
15	0.1	5.42	47.91	0.11	0.73	1.68
20	0.1	11.20	43.98	0.25	1.05	1.64
30	0.1	19.84	50.80	0.39	1.30	1.71

**Table S3.** Adsorption isotherm constants of Langmuir, Freundlich models of LaMnO<sub>3</sub>.

Langmuir		Freundlich		
q <sub>m</sub> (mg/g)	K <sub>L</sub> (L/mg)	R <sup>2</sup>	K <sub>F</sub> (L/mg)	1/n
51.3	1.44	0.993	30.08	0.189
				R <sup>2</sup> 0.925

**Table S4.** Comparison of the performance of phosphorus adsorption by different adsorbents.

Absorbents	pH	temperature	dosage	time	Conditions	Ions concentration	$q_{\max}$ (mg/g)	Selectivity (%)	Ref.
Phoslock®	-	35°C	0.23 g/L	30 h		-	10.5	-	[S1]
La-bentonite	-	25°C	2.0 g/L	48 h		-	9.06	-	[S2]
La-EDTA-Fe <sub>3</sub> O <sub>4</sub>	6.5	25°C	1.26 g/L	24 h	$C_0$ ( $\text{Cl}^-$ , $\text{NO}_3^-$ , $\text{CO}_3^{2-}$ , $\text{SO}_4^{2-}$ ) = 0.1 mM	4.19	10%-99%	[S3]	
NT-25La	-	25°C	0.1 g/L	-		-	14.0	-	[S4]
La-MOFs	6.32	25°C	0.5 g/L	24 h		-	46.3	-	[S5]
Magnetite Ferrihydrite-La	6.28	25°C	1.0 g/L	24 h	$C_0$ ( $\text{Cl}^-$ , $\text{NO}_3^-$ , $\text{CO}_3^{2-}$ , $\text{SO}_4^{2-}$ ) = 10-100 mg/L	44.8	77%-99%	[S6]	
La-Zeolite	6.0	40°C	2.0 g/L	24 h	$C_0$ ( $\text{Cl}^-$ , $\text{NO}_3^-$ , $\text{HCO}_3^-$ , $\text{SO}_4^{2-}$ ) = 0.5-20 mM	17.2	82%-99%	[S7]	
La-diatomite	5.6	25°C	0.5 g/L	24 h	$C_0$ ( $\text{Cl}^-$ , $\text{NO}_3^-$ , $\text{HCO}_3^-$ , $\text{SO}_4^{2-}$ , $\text{CO}_3^{2-}$ ) = 1, 10 mM	58.7	58%-99%	[S8]	
La-carbonate@anion exchange resin	7.0	room temperature	0.5 g/L	12 h	$C_0$ ( $\text{Cl}^-$ , $\text{NO}_3^-$ , $\text{SO}_4^{2-}$ , $\text{F}^-$ ) = 10-100 mg/L	77.43	79%-99%	[S9]	
Heated kaolinite-LaOH	-	room temperature	1.0 g/L	72 h		-	26.15	-	[S10]
MBC/Mg-La-3	6.5	25°C	0.5 g/L	72 h	$C_0$ ( $\text{Cl}^-$ , $\text{NO}_3^-$ , $\text{CO}_3^{2-}$ , $\text{SO}_4^{2-}$ ) = 100-500 mg/L	62.5	64%-99%	[S11]	
Fe-Mn binary oxide	5.6	25°C	0.2 g/L	24 h	$C_0$ ( $\text{CO}_3^{2-}$ , $\text{SO}_4^{2-}$ , $\text{Cl}^-$ ) = 1.0 and 10 mM	36.0	94%-97%	[S12]	
HMO@NS	-	25°C	0.5 g/L	24 h	$C_0$ ( $\text{NO}_3^-$ , $\text{SO}_4^{2-}$ , $\text{Cl}^-$ ) = 50-1000 mg/L	28.0	20%-79%	[S13]	
LaMnO <sub>3</sub>	5.0	room temperature	0.2 g/L	72 h	$C_0$ ( $\text{NO}_3^-$ , $\text{SO}_4^{2-}$ , $\text{Cl}^-$ ) = 50, 100 mg/L	51.3	82%-99%	this study	

**Table S5.** Kinetic fitting parameters of phosphorus adsorption by LaMnO<sub>3</sub>.

$C_0$ (mg/L)	$q_{\exp}$ (mg/g)	pseudo-first order kinetic model		pseudo-second-order kinetic model	
		$K_1$ (min <sup>-1</sup> )	$q_{e1}$ (mg/g)	$K_2$ (min <sup>-1</sup> )	$q_{e2}$ (mg/g)
2.5	12.21	0.0491	11.96	0.0295	12.63
5	22.29	0.0041	19.99	0.0018	21.62

**Table S6.** Intra-particle diffusion model of phosphorus adsorption by LaMnO<sub>3</sub>.

$C_0$ (mg/L)	$K_{d1}$	$C_1$ (mg/g)	$R^2$	$K_{d2}$	$C_2$ (mg/g)	$R^2$	$K_{d3}$	$C_3$ (mg/g)	$R^2$
2.5	1.3090	1.1069	0.9651	0.4460	7.078	0.8917	0.0138	11.736	0.5260
5	1.5327	2.4795	0.9834	0.4463	11.085	0.9814	0.1091	18.783	0.6389

**Table S7.** Change in La-O bond length after optimal.

Sample	LaFeO <sub>3</sub>				LaMnO <sub>3</sub>			
	La-O (1)	La-O (2)	La-O (3)	La-O (4)	La-O (1)	La-O (2)	La-O (3)	La-O (4)
After optimal (Å)	2.6872	2.5633	2.5082	2.5366				

**Table S8.** The main indexes of water quality of surface water from Xunsi River.

Parameter	Concentration (mg/L)	Parameter	Concentration (mg/L)	pH
Suspended Solid	36.0	$\text{PO}_4^{3-}$ -P	0.32	7.9
Conductivity ( $\mu\text{s}/\text{cm}$ )	465.0	$\text{SO}_4^{2-}$	42.5	
COD	36.0	$\text{Cl}^-$	78.1	
$\text{BOD}_5$	14.2	$\text{NO}_3^-$	52.7	
$\text{NH}_4^+$	8.4	Pb	0.06	

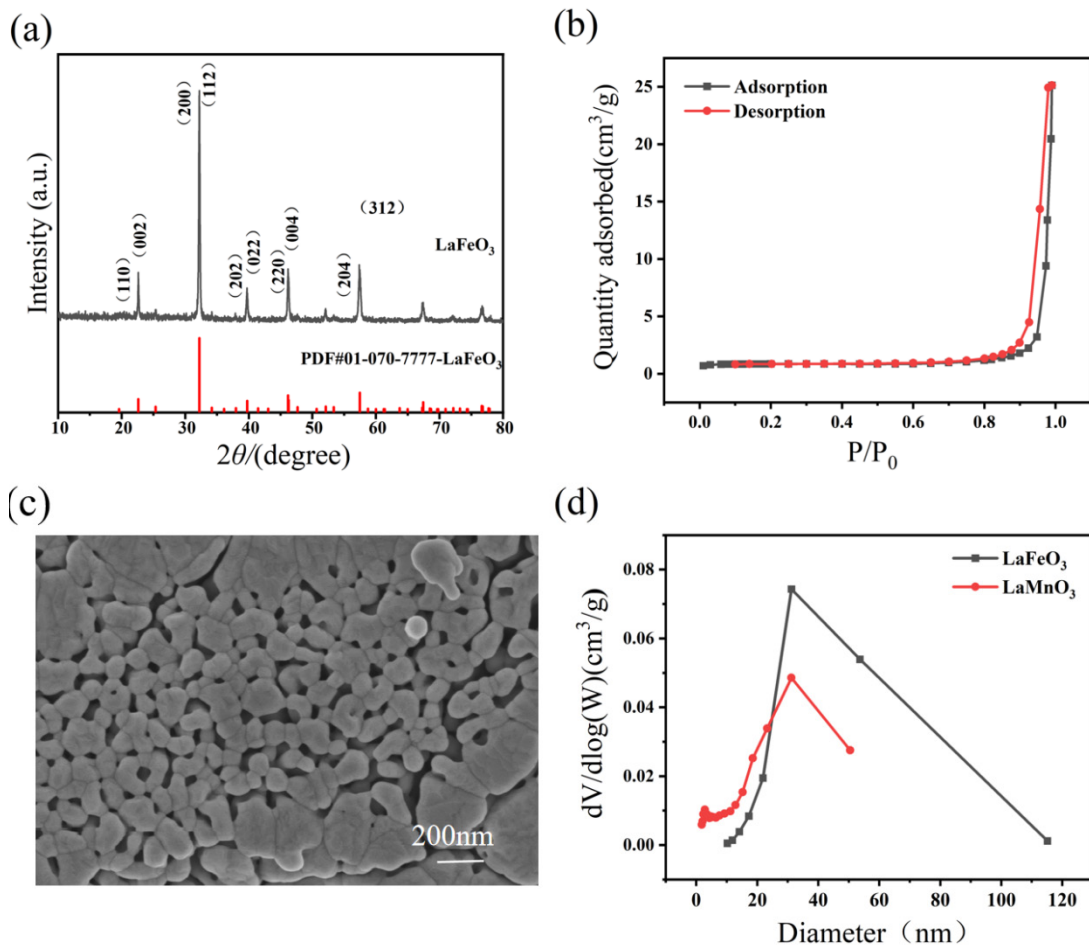


Fig.

S1.

Characterization of  $\text{LaFeO}_3$  adsorbents using (a) XRD; (b)  $\text{N}_2$  adsorption-desorption isotherms; (c) SEM; and (d) Pore distribution of  $\text{LaFeO}_3$  and  $\text{LaMnO}_3$ .

#### References

- S1. Haghseresht F, Wang S, Do DD. A novel lanthanum-modified bentonite, Phoslock, for phosphate removal from wastewaters. *Appl. Clay Sci.* 2009;46(4):369-375. <https://doi.org/10.1016/j.clay.2009.09.009>.
- S2. Li X, Chen J, Zhang Z, Kuang Y, Yang R, Wu D. Interactions of phosphate and dissolved organic carbon with lanthanum modified bentonite: Implications for the inactivation of phosphorus in lakes. *Water Res.* 2020;181:115941. <https://doi.org/10.1016/j.watres.2020.115941>.
- S3. Yang J, Zeng Q, Peng L, et al. La-EDTA coated  $\text{Fe}_3\text{O}_4$  nanomaterial: Preparation and application in removal of phosphate from water. *J. Environ. Sci.* 2013;25(2):413-418. [https://doi.org/10.1016/S1001-0742\(12\)60014-X](https://doi.org/10.1016/S1001-0742(12)60014-X).
- S4. Kuroki V, Bosco GE, Fadini PS, Mozeto AA, Cestari AR, Carvalho WA. Use of a La(III)-modified bentonite for effective phosphate removal from aqueous media. *J. Hazard. Mater.* 2014;274:124-131. <https://doi.org/10.1016/j.jhazmat.2014.03.023>.
- S5. Liu H, Guo W, Liu Z, Li X, Wang R. Effective adsorption of phosphate from aqueous solution by La-based metal-organic frameworks. *RSC Adv.* 2016;6(107):105282-105287. <https://doi.org/10.1039/C6RA24568D>.
- S6. Fu H, Yang Y, Zhu R, et al. Superior adsorption of phosphate by ferrihydrite-coated and lanthanum-decorated magnetite. *J. Colloid Interface Sci.* 2018;530:704-713. <https://doi.org/10.1016/j.jcis.2018.07.025>.
- S7. He Y, Lin H, Dong Y, Wang L. Preferable adsorption of phosphate using lanthanum-incorporated porous zeolite: Characteristics and mechanism. *Appl. Surf. Sci.* 2017;426:995-1004. <https://doi.org/10.1016/j.apsusc.2017.07.272>.
- S8. Wu Y, Li X, Yang Q, et al. Hydrated lanthanum oxide-modified diatomite as highly efficient adsorbent for low-concentration phosphate removal from secondary effluents. *J. Environ. Manage.* 2019;231:370-379. <https://doi.org/10.1016/j.jenvman.2018.10.059>.
- S9. Tee KA, Badsha MAH, Khan M, Wong KCJ, Lo IMC. Lanthanum carbonate nanoparticles confined within anion exchange resin for phosphate removal from river water: Batch and fixed-bed column study. *Process Saf. Environ. Prot.* 2022;159:640-651. <https://doi.org/10.1016/j.psep.2022.01.008>.
- S10. Zheng S, Fan J, Lu X. Heated kaolinite-La(III) hydroxide complex for effective removal of phosphate from eutrophic water. *Appl. Clay Sci.* 2023;231:106729. <https://doi.org/10.1016/j.clay.2022.106729>.
- S11. Zhu J, Rui T, You Y, Shen D, Liu T. Magnetic biochar with Mg/La modification for highly effective phosphate adsorption

- and its potential application as an algaecide and fertilizer. *Environ. Res.* 2023;231:116252. <https://doi.org/10.1016/j.envres.2023.116252>.
- S12. Zhang G, Liu H, Liu R, Qu J. Removal of Phosphate from Water by a Fe-Mn Binary Oxide Adsorbent. *J. Colloid Interface Sci.* 2009; 335 (2): 168-174. <https://doi.org/10.1016/j.jcis.2009.03.019>.
- S13. Pan B, Han F, Nie G, Wu B, He K, Lu L. New Strategy To Enhance Phosphate Removal from Water by Hydrous Manganese Oxide. *Environ. Sci. Technol.* 2014; 48 (9): 5101-5107. <https://doi.org/10.1021/es5004044>.